Microscopic analysis of astrophysical (p, γ) reaction cross sections in A=40-54

Dipti Chakraborty[1],* S. Dutta[2], G. Gangopadhyay[2], and A. Bhattacharyya[3]
Department of Physics, University of Calcutta,
92, Acharya Prafulla Chandra Road, Kolkata-700009, India

Introduction

The proton induced reactions play important role as energy generating processes in different stages of evolution of stars. The seeds in the concerned mass region A=40-54 are mainly produced in hydrostatic carbon burning and explosive oxygen burning and they take part in initiating the rp-process nucleosynthesis. This ultimately results in thermal burst in some astrophysical scenario e.g. in x-ray bursters. Study of the nucleosynthesis mechanism during various phases of stellar burning requires a complicated and coupled network calculation concerning various reaction rates or cross sections. However, very often these rates can not be measured experimentally due to instability and unavailability of targets. In such cases, theoretical extrapolation can supplement the purpose.

Methodology

The radiative (p, γ) cross sections have been studied in Hauser-Feshbach formalism with a semi-microscopic optical model potential using reaction code TALYS [1], over an energy range from 1 to 3 MeV corresponding to the Gamow window and relevant to the temperature ~ 2 GK of usual x-ray bursts. The optical potential is obtained by folding the DDM3Y NN interaction. The density dependent factor used in the folding is,

$$g(\rho) = C[1 - \beta\rho^{2/3}] \qquad (1)$$

with target radial matter densities $\rho(r)$ obtained from relativistic-mean-field (RMF) model with FSU Gold lagrangian density [2].

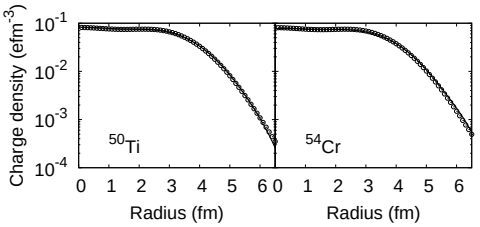

FIG. 1: Density profiles of ^{50}Ti and ^{54}Cr. Solid lines denote our results and discrete points indicate the Fourier-Bessel (FB) parameterized values.

The value of C and β are taken from nuclear matter calculation [3]. The optical model potential is constructed by taking its imaginary part identical to the real part of the folded potential. Finally, both the real and imaginary parts of OMP are renormalized with multiplicative factor of 0.9.

The cross sections $(\sigma(E))$ are then converted to astrophysical s-factors to remove the strong energy dependence, as $S(E) = E\sigma(E)e^{2\pi\eta}$. Here, E is energy in the center-of mass frame and η is Sommerfield parameter. The S-factors are then compared to available experimental data. Obviously, reasonable agreements between experiment and theory will validate our theoretical model and allow to apply and extend it to unknown regimes. Finally, we present (p, γ) rates for some important reactions as identified by Parikh *et al.*[4] and compare them with theoretical NON-SMOKER calculation [5].

Results

RMF densities play important role in folding model analysis. Hence, it is reasonable to test the success of the RMF theory. For

*Electronic address: diptichakraborty2009@gmail.com

Nucleus	B.E (MeV)		Charge radius (fm)	
	Theory	Expt.	Theory	Expt.
^{40}Ar	340.36	343.81	3.36	3.42
^{43}Ca	370.13	369.83	3.44	3.49
^{45}Sc	386.85	387.85	3.48	3.54
^{46}Ti	393.69	398.20	3.52	3.60
^{51}V	441.25	445.85	3.57	3.59
^{50}Cr	428.69	435.05	3.60	3.66

TABLE I: RMF binding energy (BE) with N_pN_n correction [6, 7] and charge radius values are compared with measurements for a few nuclei in the mass range of interest.

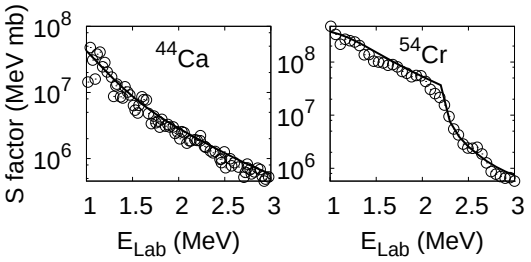

FIG. 2: Present calculation (solid line) of astrophysical S factor are compared with experimental values (discrete point) for ^{44}Ca and ^{54}Cr.

this purpose, point proton densities are convoluted with Gaussian form factor [8] to obtain charge densities and then, root mean square (rms) charge radius values. Fig. 1 shows the charge density profiles for a few nuclei in the concerned mass range with the Fourier-Bessel parameterization determined from fitting the

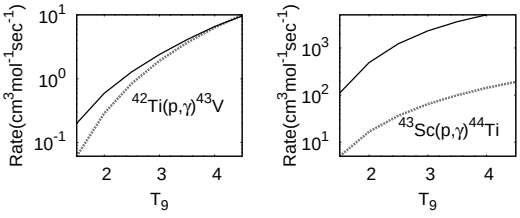

FIG. 3: Comparison of (p, γ) rate (solid line) with NON-SMOKER result (dotted curve).

experimental elastic electron scattering data [9]. In Table I, we have listed binding energies and rms charge radius values for a few nuclei with available measurements from Ref. [10] and Ref. [11], respectively. The (p, γ) astrophysical S factors for ^{44}Ca and ^{54}Cr are shown with measurements in Fig. 2. The experimental data for ^{44}Ca are from Mitchell *et al.*[12] while for ^{54}Cr are from Zyskind *et al.*[13]. Finally, Fig. 3 shows the astrophysical proton capture rates for ^{42}Ti and ^{46}V along with NON-SMOKER rates. It will be very interesting to see the effects of these rates in abundance calculations in relevent astrophysical environment.

Acknowledgments

The authors acknowledge UGC, DST, and AvH Foundation for financial support.

References

[1] A. Koning *et al.*, Proc. of the Inter. Conf. on Nucl. Data for Sci. and Technol., April 22-27, 2007, Nice, France, edited by O. Bersillon, *et al.*, (EDP Sciences, 2008) p. 211.
[2] B. G. Todd-Rutel and J. Piekarewicz, Phys. Rev. Lett. **95**, 122501 (2005).
[3] D. N. Basu, J. Phys. G: Nucl. Part. Phys. **30**, B7 (2004).
[4] A. Parikh *et al.*, The Astrophysical Journal Supplement Ser. 178,110 (2008).
[5] T. Rauscher and F. -K. Thielemann, 1998, ed Mezzacappa A., in Stellar Evolution, Stellar Explosions, and galactic Chemical Evolution. IOP Publishing, Bristol, p. 519: preprint nucl-th/9802040 Frontiére) p 525.
[6] M. Bhattacharya and G. Gangopadhyay, Phys. Lett. B **672**, 182 (2009).
[7] G. Gangopadhyay, J. Phys. G : Part. Nucl. Phys. **37**, 015108 (2010).
[8] A. Bouyssy, J. F. Mathiot, and N. Van Giai, Phys. Rev. C **36**, 380 (1987).
[9] H. De Vries *et al.*, At. Data Nucl. Data Tables **36**, 495 (1987).
[10] M. Wang, G. Audi, A. H. Wapstra, *et al.*, Chin. Phys. C **36**, 1603 (2012).
[11] I. Angeli, At. Data and Nucl. Data Tables **87**, 185 (2004).
[12] L. W. Mitchell *et al.*, Nucl. Phys. A **380**, 318 (1982).
[13] J. L. Zyskind *et al.*, Nuclear Physics A **301**, 179 (1978).